General Theory of Cross Relaxation. III. Application to Experiment*

W. J. C. GRANT
Bell Telephone Laboratories, Murray Hill, New Jersey
(Received 30 January 1964)

The theory developed in parts I and II is applied to the classical experiments of Mims and McGee, and Pershan. The predictions of the theory regarding the dependence of W_{CR} on the energy imbalance $\hbar\omega$ on concentration and on the exchange radius, as well as the prediction of the actual magnitude of W_{CR}, are confirmed in the Mims and McGee experiment on ruby. The crucial significance of near-neighbor dipole interactions, in particular, the effect of the associated power spectrum, which is quite broad and quite sensitive to crystal direction, is illustrated by application of the theory to Pershan's experiments on LiF.

INTRODUCTION

IN the preceding papers,[1] we have developed methods for calculating from first principles the cross-relaxation probability W_{CR} for processes of arbitrary complexity. The theory makes specific quantitative predictions about the dependence of W_{CR} on the number of spins participating in the process, on the energy imbalance involved, on the spin concentration, and on the existence of short-range forces. Our purpose now is to test the theory in its application to classical experiments in the field. We shall consider the experiments of Mims and McGee[2] on ruby and the experiments of Pershan[3] on LiF.

Transition probabilities are related to observable quantities through rate equations. The transient solutions of rate equations containing both cross-relaxation and spin-lattice terms have been discussed at length in a previous paper,[4] both in general and with particular reference to the experiments we shall discuss. We shall avail ourselves here of those results.

I. THE MIMS EXPERIMENT ON RUBY

We denote the four ground-state spin levels of Cr^{3+} in ruby by 1, 2, 3, 4 in order of decreasing energy. As discussed in detail in Mims' paper, the level separation (2–3) is held fixed at 7.17 kMc. The magnetic field strength and direction are varied to bring the (1–2) separation into coincidence or near coincidence with the (2–3) separation. Harmonic 1:1 coincidence occurs at about 22.3°. Levels 2 and 3 are saturated with a short pulse, and the decay of their populations is then observed. From the decays observed at a series of angles centered about 22°, the cross relaxation as a function of energy imbalance can be determined.

The details of the decay function calculated from the rate equations (see Ref. 4) depend rather critically on the assumptions one makes about the spin-lattice probabilities. Assuming equal s–l probablities W_L between all pairs of levels, the observed signal $S(t)$ is given by

$$S(t)\sim 1.5\exp(-t/\tau_1)+0.5\exp(-t/\tau_2), \quad (1a)$$

$$\tau_1^{-1}=1.5W_{CR}+4W_L, \quad (1b)$$

$$\tau_2^{-2}=4W_L. \quad (1c)$$

If one assumes s–l probabilities proportional to the energy separation of the levels one obtains

$$S(t)\sim 0.8\exp(-t/\tau_1)-0.3\exp(-t/\tau_2)+1.5\exp(-t/\tau_3), \quad (2a)$$

$$\tau_1^{-1}=2.17W_L, \quad (2b)$$

$$\tau_2^{-1}=6.28W_L, \quad (2c)$$

$$\tau_3^{-1}=1.5W_{CR}+2.23W_L. \quad (2d)$$

W_L is here taken as the s–l probability between levels 3 and 4.

When the relaxation process is dominated by cross relaxation, one obtains reasonable estimates of the cross relaxation rate regardless of detailed assumptions about s–l probabilities. It is clear, for example, that Eqs. (1a) and (2a) coalesce for times of the order of W_{CR}^{-1}, when W_{CR}/W_L becomes large.

Fortunately, many of the processes observed by Mims are indeed dominated by cross relaxation. One can fit the decay traces either by a double exponential [Eq. (1a)] or by a triple exponential [Eq. (2a)] in the region where cross relaxation is rapid. For cross-relaxation times shorter than a few msec, closely agreeing values result whether one uses equal, unequal, or infinite lattice times. The sensitivity of these particular experiments does not appear sufficient to allow consistent and quantitative interpretation of the residual trace after the fast component has been extracted.

TABLE I. C–R probabilities from Mims experiment.

ω(Mc)	τ(ms)	W_{CR}(sec^{-1})
−970	3.1	220
−670	2.3	290
−370	1.2	540
230	0.035	1900
530	5.3	125
830	22.	30

* This work was supported in part by the U. S. Army Signal Corps. under Contract DA-36-039-sc-39169.

[1] W. J. C. Grant, preceding papers, Phys. Rev. **134**, A1554 and A1565 (1964).

[2] W. B. Mims and J. D. McGee, Phys. Rev. **119**, 1233 (1960).

[3] P. S. Pershan, Phys. Rev. **117**, 109 (1960).

[4] W. J. C. Grant, Phys. Chem. Solids (July, 1964).

We show in Table I the C–R probability versus the frequency separation of the (1–2) and (2–3) transitions, as derived from the Mims experiment. The same data are also presented in Fig. 1. Because of the rapid variation of the energy imbalance ω with the field direction, and because W_{CR} becomes of the same order of magnitude as W_L for large ω, the uncertainty in W_{CR} ranges from $\sim 10\%$ for small ω to a factor of 2 or so for large ω. We note that the last two points for negative ω fall outside the main sequence. This effect is sufficiently marked so that it should probably be considered real, and we shall comment on these points later.

The theoretical expression for W_{CR}, we recall, is essentially the convolution of two functions: χ, which is the power spectrum of the dipole operator, and Φ, which in the present case is itself the convolution of the $(1 \leftrightarrow 2)$ and $(2 \leftrightarrow 3)$ resonance lines. In the following computations, we have used the form of χ given in Eq. (53) of part I. This χ function was computed using matrix elements appropriate for the magnetic field parallel to the crystal axis, and is consequently not the exactly correct function. As pointed out in part I, however, the salient features of the χ function do not depend on the detailed angular functions assumed, and Eq. (53) of part I represents a close approach to the exact function, without requiring excessive numerical computation. We may then write

$$W_{CR}=[32\pi^2\langle m^2\rangle n^2/3\hbar v L\epsilon]\Psi(\omega; L\epsilon, a). \quad (3)$$

The quantity $\langle m^2\rangle$ is the square of the transition dipole matrix element, averaged over a sphere of unit radius; the quantity L is the change in dipole energy between two flipping spins, maximized with respect to angular position, and again for unit radius; v is the average volume per lattice site; ϵ is defined by the relation $\epsilon^{-1/3}\equiv r_0=$ the effective nearest-neighbor distance; n is the fractional mole concentration of Cr^{3+} in each level; a is the half-width of Φ. $L\epsilon$ is directly related to the width of χ, [Eq. (52), part I]. The numerical constants have been so chosen that Ψ is normalized for $L\epsilon=2g^2\beta^2$.

The quantities $\langle m^2\rangle$ and L are derived from matrix elements that can be calculated precisely. The quantity a can be estimated with reasonable accuracy. In the present case, as discussed in part II, it is the width of a function obtained by convoluting the $(1 \leftrightarrow 2)$ and $(2 \leftrightarrow 3)$ resonance line shapes. (These line shapes in turn can be calculated from first principles by methods closely related to our present theory.) The quantity r_0 is a free parameter, in the sense that its theoretical prediction lies altogether outside the present theory. The value of r_0 which our theory extracts from the cross relaxation data must, however, be compared with the radius of strong exchange as determined by Statz and co-workers.[5] Exchange-coupled pairs would not, in general, be expected to participate in the two-spin cross-relaxation process, with its sharply defined resonance.

[5] L. Rimai, H. Statz, M. J. Weber, G. A. De Mars, and G. F. Koster, Phys. Rev. Letters 4, 125 (1960). H. Statz, L. Rimai, M. J. Weber, G. A. De Mars, and G. F. Koster, J. Appl. Phys. 32, 2185 (1961). M. J. Weber, L. Rimai, H. Statz, G. A. De Mars, Bull. Am. Phys. Soc. 6, 141 (1961).

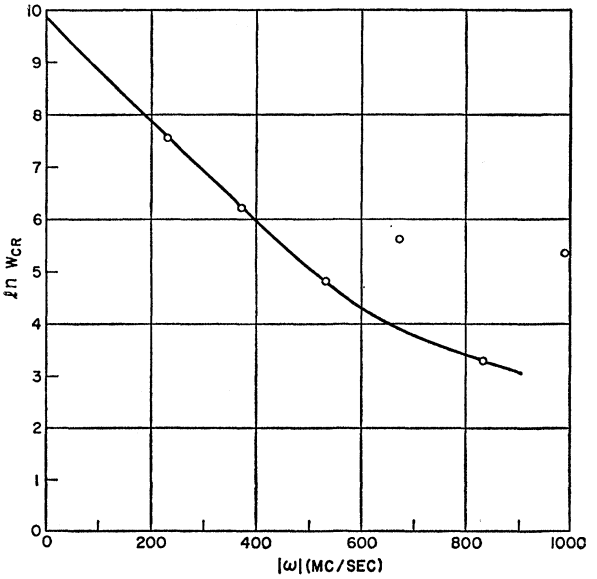

FIG. 1. Experimental data (from Mims, Ref. 2).

We first discuss the calculation of the matrix elements. These are computed from the *pair* Hamiltonian

$$\mathcal{H}_{\text{pair}}=\mathcal{H}_{\text{pair}}{}^0+\mathcal{H}_{\text{pair}}{}^{\text{dip}} \quad (4a)$$

$$\mathcal{H}_{\text{pair}}{}^0=g\beta\mathbf{H}\cdot(\mathbf{S}_1+\mathbf{S}_2)-D(S_{z1}{}^2+S_{z2}{}^2), \quad (4b)$$

$$\mathcal{H}_{\text{pair}}{}^{\text{dip}}=\frac{g^2\beta^2}{r_{12}{}^3}\left[\mathbf{S}_1\cdot\mathbf{S}_2-\frac{3(\mathbf{r}_{12}\cdot\mathbf{S}_1)(\mathbf{r}_{12}\cdot\mathbf{S}_2)}{r_{12}{}^2}\right]. \quad (4c)$$

For a particular value of $\mathbf{H}$, taking into account both its magnitude, and its direction with respect to the c axis, one diagonalizes $\mathcal{H}^0$ numerically. Then the same transformation is applied to $\mathcal{H}^{\text{dip}}$. The matrix elements relevant to a transition between the pair state (2,2) and the pair state (1,3), for example, are easily obtained from the resulting matrices. (The labels 1,2,3, refer to single-particle energy states in order of decreasing energy. They do not refer to m states, since m is not a good quantum number.) The matrix elements are complicated functions of the coordinates. For the Mims experiment they are

$$\Delta\omega\equiv\langle(1,3)|\mathcal{H}^{\text{dip}}|(1,3)\rangle-\langle(2,2)|\mathcal{H}^{\text{dip}}|(2,2)\rangle$$
$$=(g^2\beta^2/r^3)[1.36(3\cos^2\theta-1)+0.73\sin\theta\cos\theta+1.34\sin^2\theta] \quad (5)$$

$$m\equiv\langle(1.3)|\mathcal{H}^{\text{dip}}|(2,2)\rangle$$
$$=(g^2\beta^2/r^3)[0.191(3\cos^2\theta-1)+1.562\sin\theta\cos\theta+1.417\sin^2\theta]. \quad (6)$$

These matrix elements lead to the values

$$L=2.782g^2\beta^2, \quad (7)$$

$$\langle m^2\rangle=1.425g^4\beta^4, \quad (8)$$

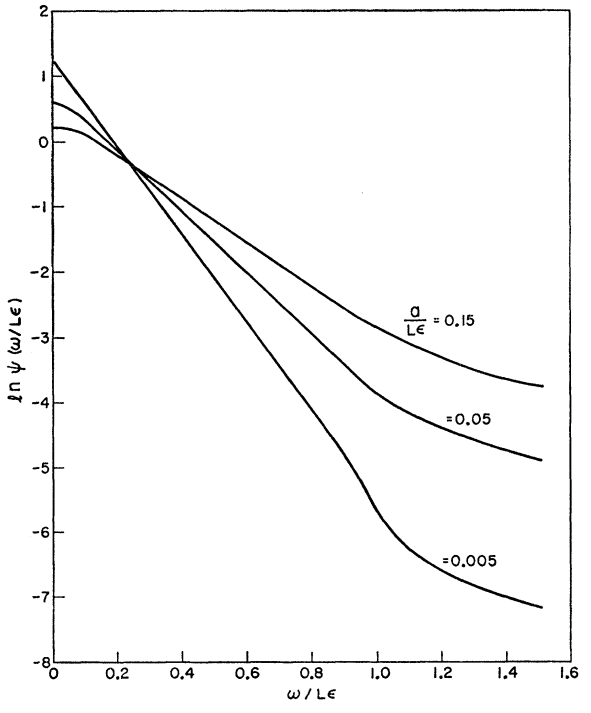

FIG. 2. ln ψ versus $\omega/L\epsilon$.

with

$$g^2\beta^2 = 5.11\times10^4 \text{ Mc}(\text{Å})^3.$$

We note that there is no need to use projection operators. Through the device of the *pair* matrix we project the appropriate portion of the dipole operator simply by inspection of the appropriate matrix elements. Of course, the use of the pair matrix allows an exact computation of the matrix elements for any operating condition, regardless of the orientation and magnitude of **H**, that is regardless of whether or not m is a good quantum number.

We next consider the dependence of W_{CR} on a and on $L\epsilon$.

Although in principle a is determined by our knowledge of resonance line shapes, in practice the situation is complicated by the presence of inhomogeneous broadening and by the complex structure not only of the total resonance line but even of its homogeneous component. At a Cr^{3+} weight concentration of 0.05%, the half-width ascribable to homogeneous broadening is about 6 Mc, and the homogeneous line shape is a Lorentzian whose falloff gradually becomes Gaussian about 1 kMc from the center frequency. The inhomogeneous broadening is a pure Gaussian of half-width about 18 Mc. The total line is the convolution of these two. It has a half-width of about 23 Mc. At the center it is dominated by the Gaussian. At frequencies more than about 60 Mc from the center it is dominated by the Lorentzian homogeneous component. In the context of cross relaxation we are usually talking about frequency separations of the order of hundreds of Mc, where the total resonance line behaves essentially like its Lorentzian homogeneous component. Very near the exact harmonic condition, cross relaxation is so rapid that the inhomogeneous line may no longer relax as a whole, in which case we are observing relaxation of individual Lorentzian spin packets rather than of the entire system. We note that the function Φ is the convolution of the $(1\leftrightarrow2)$ and $(2\leftrightarrow3)$ resonance lines, and that in convolution, Lorentzians add width algebraically, while Gaussians add width in rms fashion. One way to overcome some of these complications is to find an approximation to Ψ [Eq. (3)] from which the dependence on $L\epsilon$ can be extracted more or less independent of detailed assumptions about a, or about the shape of the function Φ.

Fortunately, such an approximation exists. If one plots $\ln\Psi$ as a function of $\omega/L\epsilon$, one obtains curves which are very closely straight lines over several orders of magnitude in Ψ. The slope of these straight lines is dependent only weakly on the shape of Φ or on the value of a. In Fig. 2, we show $\ln\Psi$ as a function of $\omega/L\epsilon$ for various values of $a/L\epsilon$, and with Φ Lorentzian. In Fig. 3, we have plotted the quantity $(a/L\epsilon)\times d\ln W_{CR}/d(\omega/L\epsilon)$ against $a/L\epsilon$. Figure 3 is, in a sense, the meeting point between theory and experiment. If $d\ln W_{CR}/d\omega$ and a are known experimentally, then Fig. 3 determines $a/L\epsilon$, and therefore ϵ. We note that a straight line of unit slope in Fig. 3 would indicate that the slope of $\ln W_{CR}$ is independent of a. For a Gaussian Φ, the acutal curve deviates negligibly from such a straight line; for a Lorentzian Φ, it deviates only slightly for small a more seriously for large a.

Our theory then predicts that $\ln W_{CR}$ should vary almost linearly with ω over several orders of magnitude (with some rounding at the very peak of the curve). The slope of this straight line yields a close estimate of the quantity ϵ, that is, of the exchange radius r_0.

This linearity is a good approximation when $a/L\epsilon$

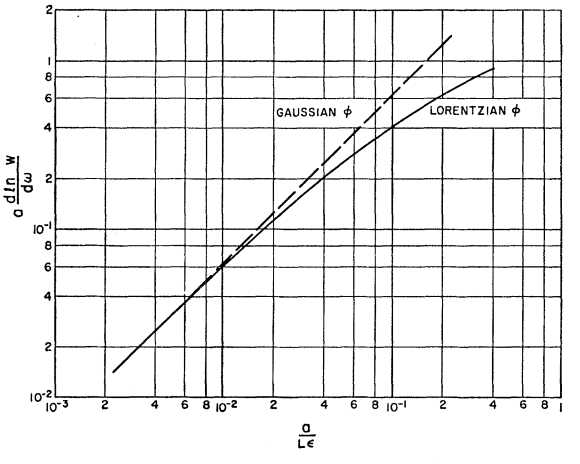

FIG. 3. $a[d(\ln\psi)/d\omega]$ versus $(a/L\epsilon)$.

is considerably smaller than unity, that is for magnetically very dilute systems. As can be seen from Fig. 1, the linear approximation to $\ln W_{CR}$ is consistent with the data of the Mims experiment.

For the Mims experiment, $d\ln W_{CR}/d\omega = 0.010$ Mc^{-1}. For a Lorentzian of half-width 12 Mc (the convolution of two Lorentzians of 6 Mc each), one obtains $r = 6.28$ Å. For a Gaussian of half-width 32 Mc (the convolution of two Gaussians of 23 Mc each) one obtains $r_0 = 6.15$ Å. In this case, therefore, it happens to make very little difference whether one uses the width of the entire resonance line or only its homogeneous component. While this is partly fortuitous, it is primarily due to insensitivity of $L\epsilon$ to the shape of Φ.

The work of Statz and co-workers[5] indicates that the exchange radius lies between about 5.5 and 6.5 Å. Thus, our value of 6.15±0.15 Å is in excellent agreement with his. We feel that such corroboration is rather encouraging in view of the startling conclusion that the first twelve or thirteen neighbor shells, or about the first fifty nearest-neighbor sites, are sufficiently exchange coupled to be excluded from this cross-relaxation process.

Because of the trick of working with the derivative of $\ln W_{CR}$, we have so far concerned ourselves exclusively with the shape of $W_{CR}(\omega)$, completely separating out the question of its magnitude. The magnitude of W_{CR} depends sharply on the concentration, and the absolute concentration is difficult to determine accurately. Nominal values of concentration are accurate within about 50%. Furthermore, there is some evidence of pronounced variations in concentration, over a scale of the order of microns, which makes the value of the true effective concentration even more obscure. In view of these uncertainties, the absolute magnitude of the cross-relaxation probability calculated by our theory, as we shall now show, agrees astonishingly well with the experiments of Mims.

Since we have already accounted for the shape of $W_{CR}(\omega)$, it suffices to calculate its magnitude at one point. For convenience, we choose the peak of the curve, $W_{CR}(0)$. The required value is given by Eq. (3), using $\Psi(0; L\epsilon, a)$. For the Mims experiment, $\Psi(0; L\epsilon, a) = 2.9$, if one assumes a Lorentzian Φ. L and $\langle m^2 \rangle$ are given by Eqs. (7) and (8). The nominal weight concentration of 0.05% corresponds to a molar concentration of 0.00034 or to a concentration per level of 8.2×10^{-5} One then computes $W_{CR}(0) = 25\,900$ sec^{-1}. Extrapolation of the curve of Fig. 1, yields $W_{CR}(0) = 18\,000$ sec^{-1}.

Even leaving out of account the considerable experimental uncertainties in the determination of the points in Fig. 1, the discrepancy between these two values can be accounted for by an actual concentration 17% below nominal. One must also bear in mind that the χ function on which this analysis is based is inexact, and that truly precise numbers cannot therefore be expected. In view of these circumstances, the agreement with experiment is excellent.

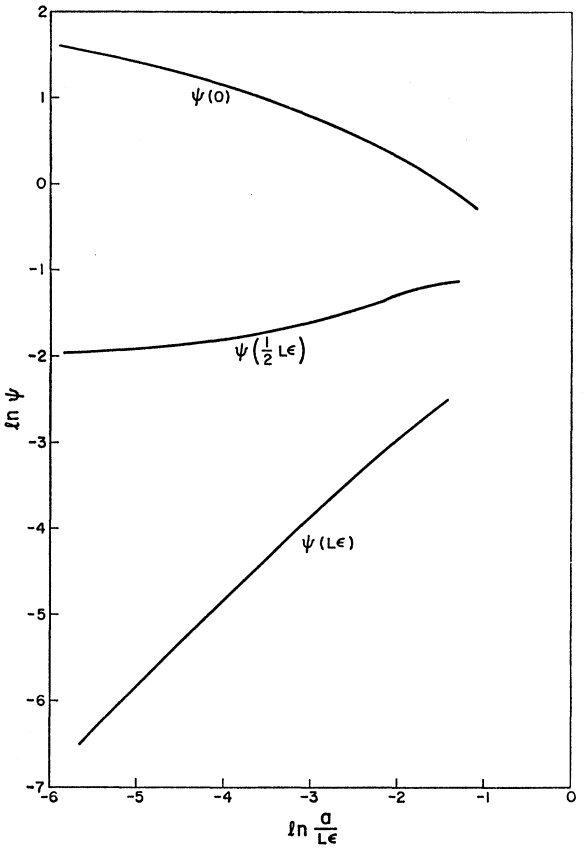

FIG. 4. $\ln\psi$ versus $\ln(a/L\epsilon)$.

We note that a linear concentration dependence of W_{CR} would give values that deviate from those observed by more than four orders of magnitude.

The interpretation of a direct measurement of the concentration dependence must be made with some care, since the concentration enters not only as a coefficient, but also determines the shape of Ψ via the parameter a. In Fig. 4 we show $\ln\psi$, evaluated at various values of ω as a function of $\ln(a/L\epsilon)$. The curves are not linear and depend drastically on the value of ω. As $a/L\epsilon$ becomes larger, the curves would all approach one another, and all would approach negative unit slope. This can be seen intuitively because ψ is normalized and approaches the normalized function Φ as $a/L\epsilon$ becomes large. The curve for $\psi(\omega = 0)$ already has a slope of -0.8 at $a/L\epsilon = 1/e$. For 0.05% ruby, $a/L\epsilon$ is about 1/20, and the slope of $\psi(0)$ is about -0.5. Since a varies almost linearly with the concentration n in this region, one would expect to measure a dependence of $n^{1.5}$ for the peak value of the cross-relaxation probability, the dependence becoming less steep at higher concentrations. Such a prediction is somewhat sanguine, since it depends not only on the precise form of χ and Φ but also on the precise values of a and $L\epsilon$.

Finally, we comment on the "stray" points in Fig. 1, which are obtained for negative values of ω. Two explanations suggest themselves: (1) Our theory predicts an asymmetry in general, if $|\Delta\omega\,\max| \neq |\Delta\omega\,\min|$. In the present case [Eq. (5)] there does exist a difference between the two extremals, the difference being about 10% of the extremum values. (2) It is also possible that the exchange-coupled pairs have a resonance about 800 Mc below the signal frequency of 7.17 kMc, that is at about 6.37 kMc. To check the reasonableness of this suggestion we have computed the pair levels assuming the conditions of the Mims experiment and an exchange energy J of 28.75 kMc (or $5D$). The antiferromagnetically coupled pairs will almost all be in the manifold for which $\mathbf{S}_1\cdot\mathbf{S}_2=9/4$. It turns out that two out of the six transitions within this manifold have an energy interval of about 6.4 kMc. The energy separations within a given $\mathbf{S}_1\cdot\mathbf{S}_2$ manifold depend only very feebly on the precise value of J, as long as J is large. For this reason our computation indicates a reasonable likelihood that the pairs will contribute to the single ion relaxation when the single ion $(1\leftrightarrow 2)$ transition is about 800 Mc below the cross-relaxation harmonic frequency.

We appear to be able, then, to explain all the features of the Mims experiment in a consistent and unified way.

Our comparison of theory with experiment might be criticized on the basis that the experimental evidence is not sufficiently copious or conclusive. For example, in Fig. 1, we have drawn a straight line on the basis of three points—an extrapolation which admittedly lacks uniqueness. Nevertheless, we can assert minimally that our calculations are consistent with the experimental data available. These data include independently the cross-relaxation decay studies, the available information regarding the structure and concentration dependence of the absorption resonance, the independent determination of the exchange radius. The area of consistency extends not only to the shapes of the functions, not only to parametric dependence, but, what is most important, to actual magnitudes. We are thus actually able to tie together, in a fully quantitative way, a substantial amount of dispersed experimental evidence.

II. PERSHAN'S EXPERIMENTS ON LiF

We next consider the cross-relaxation process in LiF, which has been investigated experimentally and theoretically by Pershan,[3] in a notable study which established decisively the existence of cross relaxation. Pershan interpreted his experiments in terms of moment theory and the convolution of Gaussian resonance lines. We shall see that our own theory leads in some circumstances to similar conclusions as Pershan's; but certain experimental features which proved anomalous in terms of his formalism find their natural place in ours.

Cross relaxation in LiF contrasts sharply in several respects with cross relaxation in ruby: (1) The process of main interest is a three-spin process involving two Li's flipping opposite one F, which requires slightly more complicated rate equations. Furthermore, neglecting quadrupole interactions, there is no zero-field splitting. The 4 Li levels are equally spaced, and transitions occur simultaneously between all pairs of adjacent levels. (2) There is no exchange interaction in LiF. This frees us from some of the major concerns in ruby, namely the extent of the exchange radius and the possible influence of exchange-coupled pairs. On the other hand, as we have seen in part II, the dipole interaction itself is now dominated by nearest, or by near, neighbors. This means that the use of a χ function based on a continuous dipole density is not justified. To obtain the correct χ we must sum over the discrete sites. (3) LiF is a magnetically concentrated system. The shape of Φ is Gaussian, and there is no question of inhomogeneous broadening.

The three-spin process can occur in any of nine mutually exclusive ways, since each of the two Li atoms can be in any one of three initial states. In addition, a second-order two-spin process can occur in which a single Li spin changes its z component by two magnetons. Two initial states are possible for this process. The decay constants for each of these relaxation modes are obtained from rate equations in Ref. 4, where it is also shown that the observed decay constant is their average.

The calculation of the matrix element governing each of these decay modes has been discussed in general in part II and with special reference to LiF in Pershan's paper.[3] We recall that each matrix element is a second-order element consisting of a sum running over six terms. The intermediate states correspond to the possiblities of any one of the three spins flipping first, and the converse. The actual computations gain considerably in simplicity and lucidity by evaluating the matrix elements of products of spin operators directly in the appropriate pair manifold.

The function $\chi(\omega)$ is given by an expression analogous to Eq. (48) of part II:

$$\chi(\omega)=2\pi\sum_{pq} M^2(\mathbf{r}_{1p},\mathbf{r}_{1q}) \times\delta[\Delta\omega_\chi(\mathbf{r}_{1p})+\Delta\omega_\chi(\mathbf{r}_{1q})+\Delta\omega_\chi(\mathbf{r}_{pq})-\omega]. \quad (9)$$

An Li is here taken as the reference atom 1; p labels all other Li atoms; and q labels the F atoms. The $\Delta\omega_\chi(\mathbf{r}_{ij})$ are the changes in dipole energy induced by the flipping of atoms i and j, as discussed in detail in part II. As discussed in part II, correlations are explicitly included through the term $\Delta\omega_\chi(\mathbf{r}_{pq})$. M^2 is the square of the transition matrix element we have just discussed. It consists of a series of terms typically of the form

$$(1/\Delta E)^2[m_1^2(\theta_{1p})m_2^2(\theta_{1q})/r_{1p}^6 r_{1q}^6]. \quad (10)$$

The symbols m^2 and ΔE have been defined and discussed in part II, Eqs. (41)–(45), and (28). In the present case

$\Delta E = g_{\mathrm{Li}}\beta H$ when an Li flips first, $\Delta E = g_{\mathrm{F}}\beta H$ when an F flips first.

We have computed the pq sums in Eq. (9) twice, once including the first neighbor shell only, and then the first two neighbor shells. The first shell consists of the nearest 6 F atoms and 12 Li atoms. The second shell contains the next 8 F atoms and 6 Li atoms. There are thus 72 terms in the first sum, 252 in the second. Each of the calculations has been done for the [001], [011], and [111] directions. It turns out that for the [001] direction the second shell already contributes only a small correction. For the other directions, the sum is also converging, but clearly has not yet reached its limit. Nevertheless, the main features of interest to us already appear clearly, as we shall see, from the summations over the first and second shells. For this reason we feel that the very steep escalation in computation time and labor, which would be necessary to carry the sum further, is unwarranted.

The appropriately weighted average of the χ functions is presented in Fig. 5, for each of the three-crystal directions. The units along the ω axis are gauss, with the correspondence $\omega = (2g_{\mathrm{Li}} - g_{\mathrm{F}})\beta H$ or 1 G = 0.697 kc. The δ functions of Eq. (9) have been smoothed by averaging over 0.6-G intervals. The ω^{-2} dependence arising from the energy denominator has been suppressed. The reason is that this factor is excluded from the convolution integral for the transition probability. That is

$$W_{CR}(\omega) \sim \frac{1}{\omega^2} \int \chi'(\omega')\Phi(\omega - \omega')d\omega', \qquad (11)$$

where χ' is ω^2 times the χ defined in Eq. (9), or in Eq. (46b) or part II.

The crucial point in Fig. 5 is that χ for the [111] direction is narrowly peaked around the origin, but χ for the [001] direction is spread out to a distance of 24 G. In part II we pointed out that the existence of large components of $\chi(\omega)$ far from the origin will result in an apparent shift of the C–R shape function away from the point of harmonic coincidence.

In the final step, convoluting χ with a Gaussian, the standard deivation σ used was 13 G for the [111] direction, 14 G for the [011] direction, and 19 G for the [001] direction. Pershan obtained a best fit using 12.7 G for the [111] direction and 14.8 G for the [011]

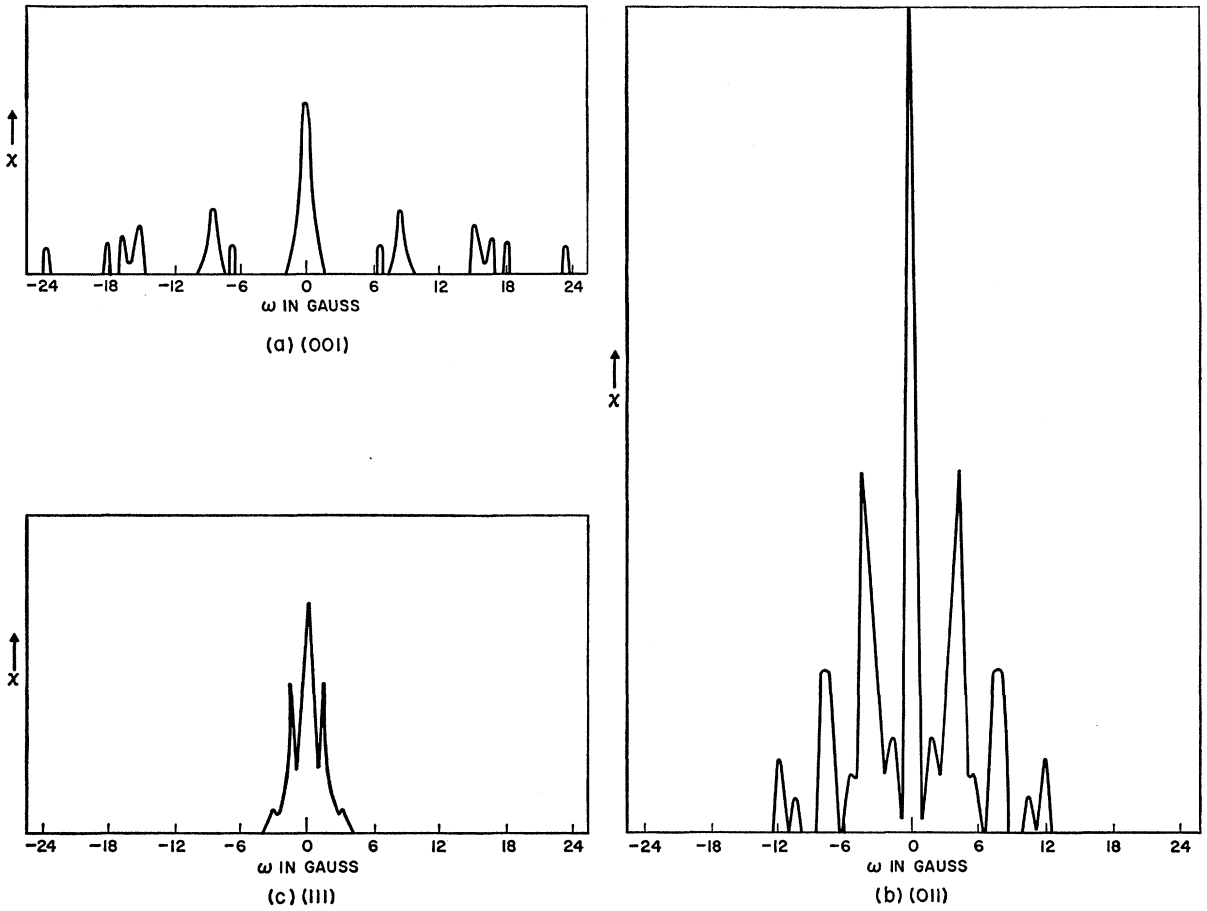

FIG. 5. $\chi(\omega)$ for LiF.

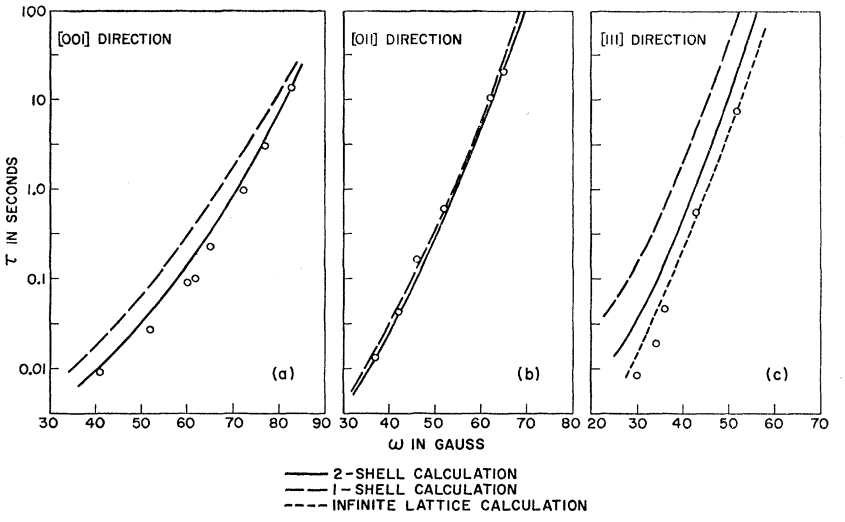

FIG. 6. C–R times for LiF.

direction. This slightly larger σ for the [011] direction compensates for his implicit approximation of χ by a δ function at the origin. For this direction, our χ does not vanish until 12 G, although it has an enormous peak at the origin. For the [001] direction, Pershan cannot match a Gaussian to the experimental data. From our point of view, it is the convolution of a Gaussian with χ that is relevant and for the [001] direction, χ extends to 24 G. At fields beyond 20 G or so, the contribution of the central peak of χ to the resultant function will be small. For example, at 65 G, the value of χ at 24 G weights 34 times as heavily in the convoluted result as does the value of χ at the origin. To a first approximation we might indeed describe the resultant W_{CR} by a Gaussian, but by a Gaussian centered at 24 G.

In Fig. 6, we show calculated and experimental C–R times. Again, the ω axis is in gauss. The experimental points shown are reproduced from Pershan's data. The solid lines show calculations based on the first two neighbor shells. The dashed lines show calculations based on the first neighbor shell only. For the [011] orientation, agreement between the calculated and experimental values are excellent. The change between the one-shell and two-shell calculations is negligible, indicating that the nearest neighbors account for practically the entire transition probability. For the [001] direction, agreement of the two-shell calculation with the data is fair, the worst discrepancy occurring at around 60 G, where the calculated times are too long by almost a factor of 2. Nevertheless, the progression from the one-shell to the two-shell approximation clearly indicates that the inclusion of further neighbors would push the calculated curve even closer to the experimental points. In this case too, the experimental numbers decisively corroborate our theory. For the [111] direction, the two-shell approximation yields times too long by about a factor of 2 over the entire observed range; the one-shell calculation yields times too long by about a factor of 10. This is to be expected. The χ function for this case consists essentially of a single sharp peak at the origin.

The contribution of the more distant neighbors is primarily in the neighborhood of the origin because of the r^{-3} dependence of $\Delta\omega$. Where the near neighbors produce no high-frequency peaks in χ, the more distant atoms can be expected to alter the magnitude of the resultant W_{CR} function, without appreciably altering its shape. To investigate this point, we have calculated C–R times for the [111] direction, extending the lattice to infinity, but replacing the lattice sums by integrals, exactly as in Eq. (46b) of part II. We have made the additional simplifying assumptions that all off-diagonal dipole matrix elements are given by $g_{\mathrm{Li}}^2\beta^2/r^3$ or $g_{\mathrm{Li}}g_{\mathrm{F}}\beta^2/r^3$, and that all the $\Delta\omega_\chi$ are zero (i.e., χ can be approximated by a single spike at the origin). The results of this calculation are shown by the dotted line in Fig. 6, and are seen to be in astonishingly close agreement with experiment.

Once again, our theory yields results consistent with Pershan's LiF data. Since for LiF, the Φ function is Gaussian, our calculation and Pershan's yield coincident results when χ is concentrated at the origin. Our theory, however, appears to extend as well to an explanation of the process in the [001] direction, where χ has a considerable spread in frequency space.

III. SUMMARY

We have applied our cross-relaxation theory to the interpretation of two classical cross-relaxation experiments. Not only the shape but also the magnitude of the calculated cross-relaxation function is consistent with the experiments of Mims and Pershan. The dependence of W_{CR}, in dilute systems, on the energy imbalance ω, on the spin concentration, and on the exchange radius is confirmed in the interpretation of the Mims experiment. The dependence of W_{CR}, in concentrated systems,

on interactions with near neighbors, and its associated spread and displacement in frequency is confirmed in the interpretation of Pershan's experiment.

IV. COMPUTATIONAL NOTE

This study has involved a sizeable mass of numerical detail. The generation and manipulation of large pair matrices, the tabulation of the various χ functions, the evaluation of different convolution integrals, to mention only the more obvious computational tasks, have had to be performed on a mass-production basis. The use of the Bell Telephone Laboratories IBM-7090 computer has proved indispensable. The computer programs were written by the author.

PHYSICAL REVIEW VOLUME 134, NUMBER 6A 15 JUNE 1964

Molecular Field Model and the Magnetization of YIG*

ELMER E. ANDERSON
U. S. Naval Ordnance Laboratory, White Oak, Maryland
and
The University of Maryland, College Park, Maryland
(Received 7 January 1964)

The susceptibility and magnetization of YIG of high purity have been measured from 4.2 to 650°K by means of a precision vacuum balance. The spontaneous magnetization has a saturation value of 37.90 emu/g at 4.2°K and 27.40 emu/g at 292°K. The Curie point is at 559°K as determined by both the vanishing of the spontaneous moment and the discontinuity in the susceptibility curve. Using a program written for the IBM 7090, the molecular field coefficients were determined by fitting the experimental total magnetization curve. The sublattice magnetizations and the exchange interactions are calculated and compared with other results. On the basis of the molecular field model the intrasublattice interactions must be larger than previously supposed.

INTRODUCTION

ACCURATE sublattice magnetization data are required for an adequate description of such quantities as the magnetic anisotropy and magnetostriction in ferrimagnetics. The first calculations of the sublattice magnetizations in the garnets were made by Pauthenet in 1957 based on the molecular field model.[1] Though his results have been the only ones available it has long been apparent that they could be improved upon by using purer samples and a better method of solving the molecular field equations. An alternative approach is to measure the magnetization of a sublattice indirectly by observing the magnetic resonance frequency or the Mössbauer absorption of nuclei situated in that sublattice. This was first done for YIG by Solomon[2] and Robert[3] and has been repeated by several others,[4–9] some of whose results will be discussed in a later section. It may be said here, however, that the NMR measurements have not been extended to sufficiently high temperatures to represent any real improvement over Pauthenet's results.

In this present study the total spontaneous magnetization was obtained by subtracting the field-dependent magnetization from the measured values for high-purity YIG over the temperature range from 4.2 to 650°K. These values of the spontaneous magnetization were fed into a program written for the IBM 7090 by Gerhard Heiche of this laboratory and the molecular field equations were solved for all temperatures. The molecular field coefficients computed in this manner are used to calculate the sublattice magnetizations and the exchange interaction energies for YIG. Similar results for the three sublattice garnets will be the subject of a separate paper.

EXPERIMENTAL APPARATUS

The technique used for the measurements reported here is a modification of the Curie method.[10] Briefly, the sample is placed in a magnetic field having a large gradient and the force on the sample is measured by a sensitive balance. The essential unit is an automatic vacuum balance and recorder which can weigh accurately to 3×10^{-5} g. A quartz sample holder is suspended from one pan of the balance so that the sample

* This work is an excerpt from a thesis submitted to the University of Maryland in partial fulfillment of the requirements for the degree of Doctor of Philosophy. The research was performed at the U. S. Naval Ordnance Laboratory.

[1] R. Pauthenet, Ann. Phys. (Paris) **3**, 424 (1958).
[2] I. Solomon, Compt. Rend. **251**, 2675 (1960).
[3] C. Robert, Compt. Rend. **251**, 2684 (1960).
[4] G. K. Wertheim, Phys. Rev. Letters **4**, 403 (1960); J. Appl. Phys. **32**, 110S (1961).
[5] C. Alf and G. K. Wertheim, Bull. Am. Phys. Soc. **5**, 428 (1960).
[6] E. L. Boyd, L. J. Bruner, J. I. Budnick, and R. J. Blume, Bull. Am. Phys. Soc. **6**, 159 (1961).
[7] S. Ogawa and S. Morimoto, J. Phys. Soc. Japan **17**, 654 (1962).
[8] L. D. Khoi and M. Buyle-Bodin, Compt. Rend. **253**, 2514 (1961).
[9] E. L. Boyd, V. L. Moruzzi, and J. S. Smart, J. Appl. Phys. **34**, 3049 (1963).
[10] P. Curie, Ann. Chim. Phys. (7) **5**, 289 (1895).